IEEE Access
Multidisciplinary | Rapid Review | Open Access Journal

Received April 19, 2022, accepted May 8, 2022, date of publication May 30, 2022, date of current version June 6, 2022.

Digital Object Identifier 10.1109/ACCESS.2022.3178999

A System Deployment Model of Multi-CCD Automatic Optical Inspection for Economical Operations

KUNG-JENG WANG, (Member, IEEE), AND YI-CHENG QIU
Department of Industrial Management, National Taiwan University of Science and Technology, Taipei 10607, Taiwan
Corresponding author: Kung-Jeng Wang (kjwang@mail.ntust.edu.tw)

ABSTRACT Overkill and leakage are common problems in automated optical inspection (AOI) systems that have harmed firms to devote in intensive manual reinspection and seek the best CCD setting, resulting in more costly and less effective AOI operations. This study proposed a two-stage AOI based inspection system deployment model of multi-charge coupled device (CCD) for cost reduction; that is, the strictness decision model of a single CCD in the operational stage and switch on/off decision model of a set of CCDs in the strategic stage. The strictness decision model identifies the best strictness level of individual CCD by analyzing a confusion matrix according to the true defect rate of products. The multi-CCD switch decision model suggests the best switch on/off decision of multiple CCDs. Experiments in an electrical connector manufacturing plant revealed that the total inspection cost was the lowest when the strictness level was set close to the true defect rate. The best multi-CCD on/off strategy was more cost-effective than was the all CCDs-on mode under various strictness settings, by cost reduction up to 23.49%. In general, the proposed two-stage model achieves flexible multi-CCD settings of AOI systems and operations at a low cost. The proposed model can be extended to different applications of overkill and leakage problems. In this study, the proposed VGG-like convent five-layer convolution model learns from the experience of quality re-inspection personnel, which can be applied to the re-inspection line to identify AOI as defective images for re-inspection. The best accuracy reaches 99.21%.

INDEX TERMS Automated optical inspection, charge coupled device, confusion matrix, cost-effective analysis, inspection system deployment, Type I & II errors, CNN.

I. INTRODUCTION

The information technology (IT) industry has prompted to microminimizing electronic component [1], [2] that fabricates components with dimensions less than 10 mm and precisions of 5-20 μm, such as integrated circuits (ICs), printed circuit boards (PCBs), liquid-crystal displays, ball grid arrays, electronic communication components, and electrical connectors. These components must undergo detailed inspections [3] requiring the use of automated optical inspection (AOI) instead of conventional human inspection techniques that suffer several disadvantages, such as being time-consuming, inaccurate, and highly reliant on subjectivity [4], [5].

AOI is known for its high recognition rate, noncontact inspection, and impressive mechanical flexibility [6], [7]. However, efficient AOI systems should be flexible and lean to adapt to changing quality status [2], [8], [9].

An AOI system with multi-charge coupled devices (CCDs) is preferable for inspecting electronic products due to the need for multi-defect inspections [10]. However, such a system, usually empowered by deep learning technologies, is costly and time-consuming when all CCDs are turned on simultaneously [11]. Moreover, AOI is limited by the need to make constant adjustments according to changing quality status. These adjustments are necessary to maintain a low false call rate when performing quality checks; if not appropriately adjusted, the inspection effectiveness may be deteriorated and the process delayed [12], [13]. The existing AOI process depends on quality engineers to calibrate inspection procedures and classify defective goods, which

The associate editor coordinating the review of this manuscript and approving it for publication was Muhammad Ali Babar.

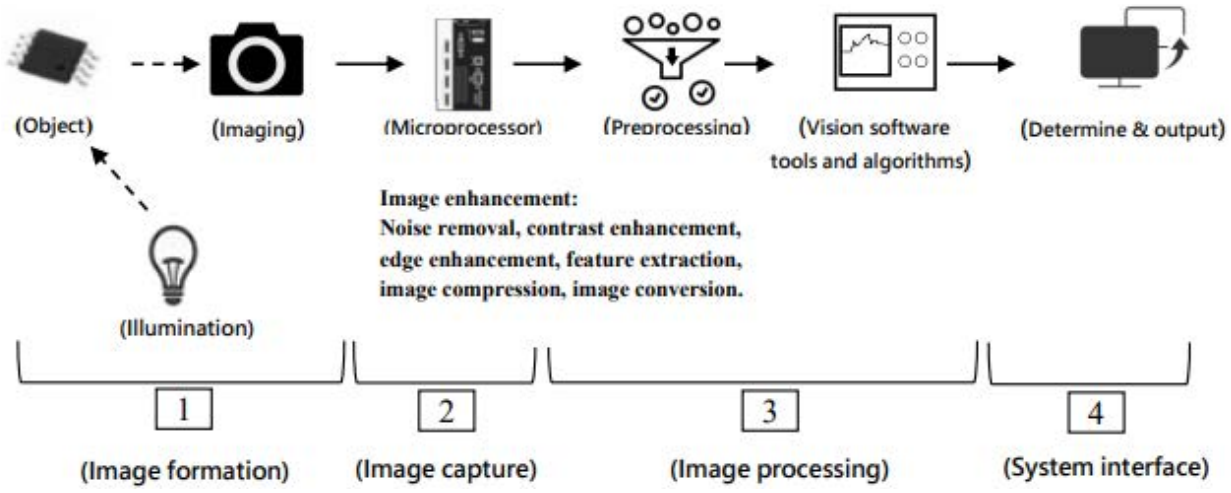

FIGURE 1. Image recognition process of an AOI system.

may lead to severe errors [12]. For example, when the AOI threshold is improperly set or if product quality varies considerably, the AOI system is more likely to make false calls, resulting in overkills (i.e., Type I error) or defect leakage (i.e., Type II error). Overkills may require additional inspections [14] that increase labor and rework costs [15], whereas leakage may cause defective goods to be sold to customers, resulting in an increased customer complaint cost [16]. Therefore, solutions must be developed for the optimization of multi-CCD AOI systems to reduce inspection costs [17], [18].

The present study developed a multi-CCD AOI deployment model; at the operational level of the product line, the model provides suggestions for AOI engineers to first, properly adjust CCD- threshold parameters according to the product defect rate in question and second, reduce overkills and leakage caused by AOI false calls. At the strategic level, the model can recommend the best multi-CCD switch configurations according to various yields, thereby lowering the total inspection cost.

II. LITERATURE SURVEY

A. TYPES OF AOI

AOI involves the use of image processing and machine vision technologies to compare the device under test (DUT) with a standard image and then verify whether the DUT meets the standard and has any defects (refer to Figure 1). The AOI system guides samples to the inspection platform, on which a CCD captures the image of each sample. The system then acquires eigenvalues through noise filtering and performs an image matching analysis to determine whether the sample is defective [1], [19].

AOI systems can be divided into rule-based and learning-based systems according to their defect classification methods [3], [5], [20]. A rule-based system classifies defects based on specific rules and thresholds [21], [22], yet the classification accuracy of such system is low. To solve this problem, machine learning techniques (e.g., convolutional neural networks) are adopted to improve its inspection rate and accuracy [23], [24].

B. AOI FALSE CALLS

AOI false calls can be divided into overkills and leakage. An overkill occurs when the system mistakenly determines a product as being defective because of excessively high inspection standards [14], [25]. Conversely, leakage occurs when the AOI standards are excessively low, causing the system to wrongly identify a defective unit as a non-defective one. Therefore, a balanced AOI parameter design is an essential factor affecting inspection costs.

III. METHOD

A. MODEL FRAMEWORK

In this study, a multi-CCD AOI deployment decision system was proposed. The system comprises two decision-making levels that facilitate inspection cost reduction (Table 1). In this system, (i) the operational level optimizes settings related to CCD strictness for various defect rate requirements using a confusion matrix, and (ii) the strategic level, with the best multi-CCD switch model, facilitates switch decision-making that identifies the best multi-CCD configuration.

This model can be applied to a set of CCDs. The proposed AOI system is depicted in Figure 2. The model is plugged into the AOI system, and apply in the quality inspection process. The CCDs strictness algorithm adjusts the strictness parameter and the AOI pixel limit range. In Stage-II, the web plug-in function assists quality personnel to set the AOI CCDs switch on/off.

The factory manufacturing execution system (MES) connects the output of the proposed system to improve the defect detection efficiency. In this study, the CNN model learns from the experience of quality re-inspection personnel, which can be applied to the re-inspection line to identify AOI as defective images of re-inspection.

TABLE 1. Proposed two-stage multi-CCD deployment decision model.

CCD deployment decision model	Input	Output
I. The CCD strictness model	1. Inspection cost 2. CCD false call rate (%) 3. True defect rate (%) 4. True defect rate due to individual CCD (%)	Best CCD strictness level of single CCDs
II. The multi-CCD switch model	1. Inspection cost 2. CCD false call rate (%) 3. True defect rate (%) 4. True defect rate due to individual CCD (%)	Best multi-CCD switch decision

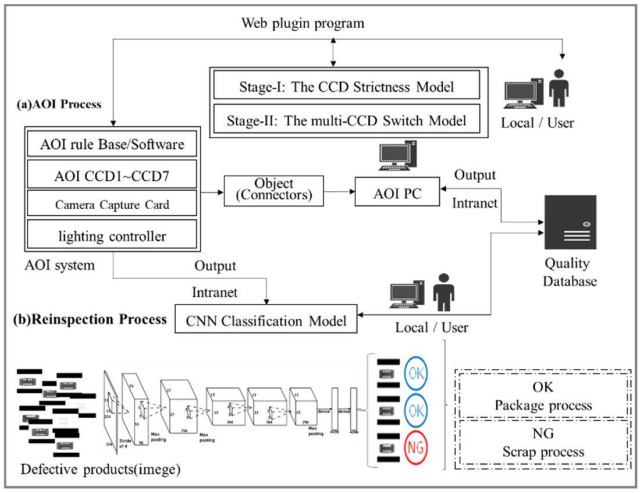

FIGURE 2. AOI system technology application framework.

B. THE STRICTNESS DECISION MODEL FOR INDIVIDUAL CCD

Figure 3 presents the schematic model of the two-stage model. Goods from the manufacturing process are examined by AOI and classified into four categories, as indicated in the confusion table. Those 'inspect positive' goods are delivered to the sequent packing process, while those 'inspect negative' goods are reexamined by human inspectors to screen scraps. When the CCD strictness level was high, overkills were likely, causing the Type I reinspection cost to exceed Type II defect leakage cost.

The AOI system under investigation consists of 7 CCDs. The two-stage model is applied to CCD1-CCD7, and the output results are fed back to the AOI system. In this study, the decision-making process is depicted in Figure3. Stage-I is the CCD strictness model. According to the result of analyzing the defect image, the CCD strictness model identifies the best strictness level of individual CCD by analyzing a confusion matrix according to true defect rate of products. Stage-II is the multi-CCD switch model. The multi-CCD switch decision model suggests the best switch on/off decision of multiple CCDs. The CNN neural network was used to

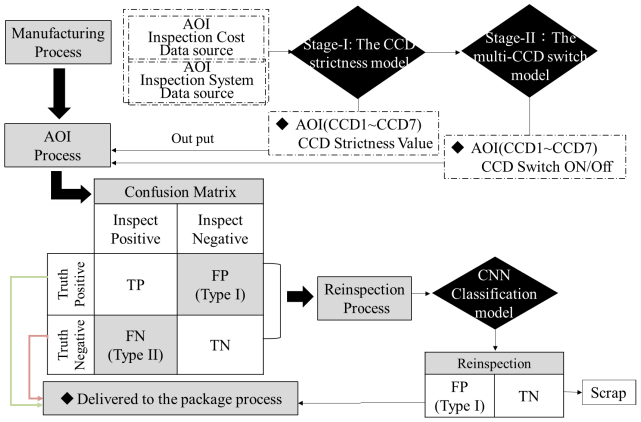

FIGURE 3. The two-stage model process structure.

analyze the defect image and establish a CNN classification model. Deep learning can be used to assist the existing AOI architecture and provide a new option for back-end quality re-inspection to replace the human inspection and identify defects, improve production efficiency.

Figure 4(a) presents the computational procedure of the CCD strictness decision model at different CCD strictness levels by permutation search, and Figure 4(b) depicts the 7 steps of the confusion table computation of the total cost of AOI. The terms used in the present model are defined as follows. Type I error occurs when a non-defective unit is mistakenly regarded as a defective one, also known as a false positive. Type II error occurs when the system fails to identify a defective good and considers it a non-defective one, also known as a false negative. CCD false call rate (%) is the ratio of the number of single-CCD false calls to that of defective goods captured by a single CCD. True defect rate (%) is the quotient that is the number of identified defective goods divided by the sum indicating the target delivery quantity. True defect rate due to this CCD (%) is the ratio of the number of defective goods captured by a single CCD to that of system-captured defective goods. CCD strictness is the inspection thresholds defined by the AOI equipment.

Input

(1) System parameters:

- True defect rate (%) //DUT true defect rate in steady-state of the production line
- Input quantity (pcs per hour) //production batch
- True defect rate due to this CCD (%) // True defect rate detected by this CCD in steady-state of the production line
- CCD false call rate (%) //CCD optical quality level of this CCD

(2) Inspection unit cost:

- Inspection cost per unit: number of final products inspected by the AOI system
- Whole-plant prevention cost: Cost of preventing the occurrence of defective goods

- AOI equipment cost: Cost of purchasing AOI equipment
- Average identification cost: Cost of defining products as defective goods
- Human inspection cost: Labor cost of inspection staff
- Internal failure cost: Cost incurred from poor quality prior to the products being delivered to customers
- Reinspection equipment cost: Cost of reinspection equipment
- Reinspection labor cost: Cost of reinspection staff
- External failure cost: External cost incurred due to products failing to meet customer requirements

Procedure

For strictness level from 0% to 100%

DO

Step 1: Establish a confusion matrix of inspection costs of a CCD.

(1) Defect = Input × true defect rate

(2) Reject = Input × CCD strictness × CCD-captured defect rate

(3) FP (Type I) = Reject × CCD inaccuracy level

(4) TN = Reject − FP

(5) FN (Type II) = Defect − TN

(6) Accept = Input − Reject

(7) TP = Accept − FN

Step 2: Calculate the total cost.

(1) Total initial inspection cost = (AOI equipment inspection cost per unit + prevention cost per unit) × quantity of products manufactured per hour + (human inspection cost per unit + identification cost per unit) × (TN + FP)

(2) Total reinspection cost (i.e., cost of Type I error) = (reinspection labor cost per unit + reinspection equipment cost per unit) × FP

(3) Cost of defect leakage (i.e., cost of Type II error) = external failure cost per unit (i.e., compensation due to damaged goods, reworking labor cost, implicit cost of reputational damage) × FN

(4) Total cost of defective goods (rework and scrapping costs) = internal failure cost per unit × (TN + FP)

(5) Total cost = (1) total initial inspection cost + (2) total reinspection cost (i.e., cost of Type I error) + (3) total cost of defect leakage (i.e., cost of Type II error) + (4) total cost of defective goods

ENDDO

Output

The best CCD strictness setting to minimize the total cost of this CCD

C. THE SWITCH DECISION MODEL FOR THE MULTI-CCD AOI SYSTEM

To minimize total inspection cost, the proposed multi-CCD switch model identifies the best multi-CCD switch decision at various requirements defined by true defect rate and strictness. Figure 5 presents the computation procedure. The process begins with the computation of the strictness decision model for each CCD to determine the best strict level of

(a) Computational procedure of the CCD strictness decision model

Confusion Table		AOI Detection		
		No Defect(+)	Has Defect(-)	
Truth	Positive(+)	TP =Accept-FN (# 7)	FP(TypeI) =Reject* CCD inaccuracy level (# 3)	
	Negative(-)	FN(Type II) = Defect-TN (# 5)	TN =Reject-FP (# 4)	Defect =Input*Defect Rate (# 1)
		Accept =Input-Reject (# 6)	Reject= Input × CCD strictness × CCD-captured defect rate (# 2)	

- Cost of Type I error (misjudging a nondefective unit as a defective one) = AOI reinspection equipment cost per unit + reinspection labor cost per unit
- Cost of Type II error (sale of defective goods to customers) = Cost of external failure per unit
- Defect rate (%) = $\frac{\text{Number of defective goods captured by each } CCD}{\text{Total number of defective goods captured by all CCDs}}$
- CCD inaccuracy level (%) = $\frac{FP}{TN+FP}$
- True yield (%) = $\frac{TP+FP}{SUM}$
- True defect rate (%) = 1 − $\frac{TP+FP}{SUM}$

(b) Seven steps of confusion table computation

FIGURE 4. Computational procedure of proposed CCD strictness decision model.

Input

(1) System parameters:
- same as the CCD strictness model
- The best CCD strictness of each CCD (%) // computed by the CCD strictness model

(2) Inspection unit cost:
- same as the CCD strictness model

Procedure

For each CCD

DO

Step 1: Calculate the total AOI cost: same as the CCD strictness model

Step 2: Calculate the total cost of closing a CCD
- Total cost of closing CCD = AOI CCD Type II error cost = unit external failure cost * (FN + TN)

Step 3: Cost comparison
- Calculate the cost difference caused by CCD opening and closing
- If (total cost of CCD opening < total cost of CCD closing, 0,1) set CCD to 1 (opening), otherwise set CCD to 0 (closing)

END DO

Output

The best multi-CCD switch on/off decision and corresponding total cost

FIGURE 5. Computational procedure of the proposed multi-CCD switch model.

single CCDs. The cost of a CCD to turn on or off is then iteratively calculated by permutation search to decide the multi-CDD switch decision.

D. CNN CLASSIFICATION MODEL ALGORITHM

The VGG-like convent five-layer convolution model, 32 convolution filters of size 3 × 3 each, 100 × 100 images with 3 channels for input data, is adopted as the CNN model. The batch size is 32. Epoche = 20. SGD (stochastic gradient decent) is the optimization method for this experiment. The learning rate is set to 0.1, and the attenuation value (decay) is 1e-6. The above parameter settings are all VGG official settings. The photo type is set to grayscale because the images in this case is black and white. Figure 6 is the Pseudo code of the first three stages of the CNN algorithm.

Pseudo code of CNN Classification model

Input: *Images of CCD4 and CCD5.*
Output: *Classification and probability of class.*
Parameters:
Batch size → 32 *– the size of samples for networks*
Numepochs → 20 *– the number in training algorithm*
Target size → (100,100) *– the dimensions to which all images found will be resized*
Color mode → grayscale *– the images will be converted to have 1 or 3 color channels*
Class mode → categorical *– mode for yielding the targets*

Step 1: Read image data.
- The image should be classed by label.
- The image would be adjusted by the parameters.

Step 2: Set CNN layers with input layer, hidden layer and output layer.
- Set input shape.
- Set Convolution, pooling, flatten and dropout layer in hidden layer.
- Adjust parameter in dense layer as the number of class.

Step 3: Employ train samples and start to train.
- Cnn=cnntrain(cnn, train_x, train_y);
- SGD will be used as the optimizer.
- Save the training model.

Step 4: Employ test samples and start to test.
- [class, probability]=cnntest(cnn, test_x, test_y);

FIGURE 6. **Algorithm of CNN classification model.**

The products are classified as Good and No_Good by an CNN classification model. The number of input data (images) is 2,000. The original images are the jpg format of Height: 2050 pixels and Width: 2432 pixels. The examples of good and defective products are displayed in Figure 7. For example, the lens angle of CCD4 is vertical of the back side. Class_A shows excess glue in the metal HD, and class_I shows excess metal at the pins. Before feeding the images into the CNN model, the black border of the image is cropped to detect defects easily. The cropped images are jpg format of Height: 728 pixels and Width: 1052 pixels. The shot angle of CCD5 is vertical of the front side with backlighting. Class_L is the extra metal scrap on the plastic body, and class_N is the extra plastic material on the edge of the product. The original images are the jpg format of Height: 2050 pixels and Width: 2432 pixels. The cropped images are jpg format of Height: 1972 pixels and Width: 1059 pixels.

IV. EXPERIMENT AND DISCUSSION

The experiment was conducted in an electrical connector manufacturing plant equipped with a multi-CCD AOI system using deep learning algorithms. The algorithm is implemented by Python and the tensorflow program set was applied to support a variety of applications in the present study, with a focus on training and inference on deep neural networks [26]. The program is run on Intel® Core™ i7 Processor 2.5GHz (8 cores), NVIDIA® GeForce® 6GB, and 1TB SATA HDD, under Windows 10 operating systems. As a DUT was regarded as defective by the system, the good was subjected to quality reinspection performed by reinspection staff, who returned the sample to the production line if its quality was acceptable. The adopted AOI system, comprising seven CCDs, inspected 112,385 pieces of components per day.

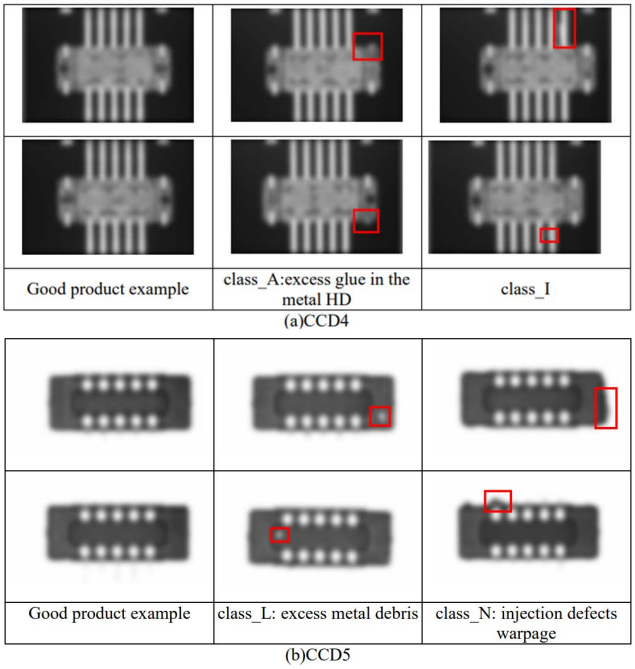

FIGURE 7. **The examples of CCD4 and CCD5.**

TABLE 2. **CCD-captured defect rate and false call rate.**

CCD name	CCD-captured	False call rate (%)
CCD1	8.21%	1.39%
CCD2	9.16%	21.64%
CCD3	22.55%	2.25%
CCD4	20.17%	15.12%
CCD5	13.44%	3.97%
CCD6	13.05%	13.24%
CCD7	13.41%	21.52%
	Total: 100.00%	Mean: 11.31%

The K-fold cross validation is applied in the experiment. K = 10 means that the data is divided into 10 equal parts. 80% of the data is used as the training set, 10% is used as the validate data set, and 10% is used as the testing set. Each part of data will be used as the testing set three times, so a total of 30 experiments were performed.

The defect rate and false call rate are listed in Table 2. Among all CCDs, CCD3 had the highest defect rate (22.55%), whereas CCD2 had the highest falste call rate (21.64%); the AOI system yielded an average false case rate of 11.31%. The results help quality operators adjust threshold parameters at the operational level, thereby reducing the probability of overkills and leakage.

The description of CCD1-7 detection items examined by the proposed AOI system with deep learning algorithm is shown in Figure 8. The sample results of the CCD4 and CCD5, which are classified into good and no good classes,

Camera	Angle of shot	Detect item	Image in AOI
CCD1	30° on the side	excess metal at the pins Inside	
CCD2	30° on the side	excess metal at the pins Inside edges	
CCD3	Vertical above (Frontlighting)	excess metal at the pins	
CCD4	Vertical below	excess metal at the pins	
		excess glue in the metal HD	
CCD5	Vertical above (Backlighting)	excess metal debris	
		injection defects warpage	
CCD6	Side parallel	excess metal at the pins Outside	
CCD7	Side parallel	excess metal at the pins Inside edges	

FIGURE 8. The detect patterns of components.

TABLE 3. Sample result of CNN classification model.

Item	CCD4	CCD5
Average accuracy(%)	97.83	90.15
Best accuracy(%)	99.21	98.45
Worst accuracy(%)	89.68	80.31

are listed in Table 3. The data was divided into 10 parts and applied to 30 times cross-validation to obtain the results. The average accuracy of CCD 4 and CCD5 are 97.83% and 90.15% respectively. The result show that the proposed CNN classification is highly stable.

A. RESULT OF THE STRICTNESS DECISION MODEL

Taking CCD1 as an example, Table 4(c) details the calculation of cost per unit given a true defect rate of 7%, and Table 4(a) presents the confusion matrix for cost calculation. When all CCDs were turned on with a true defect rate of 7%, the total inspection cost on CCD1 was $ 61.36; the individual costs are detailed in Table 4(b). The CCD strictness model calculated total inspection costs under various true defect rates and strictness rates when all CCDs were turned on (Table 5). The cost information is obtained through the cost accounting system. The quality inspection data is obtained through the AOI supervisory control and data acquisition (SCADA) system. Related data is used to measure yield rate changes in real-time.

Table 5 presents the best strictness given a true defect rate, denoting as a marked number. It reveals that, when the

TABLE 4. Illustration of the CCD strictness model for CCD1.

(a) Confusion table for cost calculation

	AOI		
	No Defect	Has Defect	
Positive	TP=Accept-FN 5313.54 = 5681.16-367.62(Step 7)	FP (Type I) = Reject ×CCD1 false call rate 0.46 = 32.84 * 1.39% (Step 3)	
Negative	FN(TypeII)=defect- TN 367.62=400-32.38 (step 5)	TN = Reject-FP 32.38 = 32.84–0.46(Step 4)	Defect = Input × defect rate 400=5714*7% (Step 1)
	Accept = Input − Reject 5681.16 =5714-32.84 (Step 6)	Reject = defect × CCD1-captured defect rate 32.84 =400*8.21% (Step 2)	

Unit: RMB Per Hour

(b) Results of total cost calculation for CCD1 (given true defect rate = 7%)

Initial inspection cost	5.99
Cost of Type I error	0.12
Cost of Type II error	11.95
Cost of defectives	43.30
Total cost	61.36

Unit: RMB Per Hour

(c) Calculation of cost (in RMB) per unit

Number of units inspected per hour (5714 pieces/h) = productivity (60,000 pieces)/production time (10.5 h) (1)

True defect rate of the company's DUTs = 7%; CCD strictness = 7% (2)

AOI equipment cost per unit: 0.00012/piece/number of CCDs = $\left[\frac{AOI\ equipment\ cost\ (300{,}000)}{250\ days \times 21\ h \times 10\ years}\right]$ /7 CCDs/7,000 pieces/h (3)

Prevention cost per unit: 0.00088/piece/number of CCDs = $\left[\frac{Average\ whole-plant\ prevention\ cost\ in\ January–September\ (18{,}054)}{20\ days \times 21\ h}\right]$ /7 CCDs/7,000 pieces/h (4)

Human inspection cost per unit: 0.00238/piece= $\left[\frac{Human\ inspection\ cost\ (7{,}000)}{20\ days \times 10.5\ h}\right]$ / 14,000 pieces (2 AOI machines)/h (5)

Identification cost per unit: 0.007/piece/number of CCDs = $\left[\frac{Average\ whole-plant\ identification\ cost\ in\ January–September\ (145{,}761)}{20\ days \times 21\ h}\right]$/ $7CCDs$/7,000 pieces/h (6)

Reinspection labor cost per unit: 0.267/piece/number of CCDs = $\left[\frac{Reinspection\ labor\ cost\ (7{,}000) * 4\ people}{20d \times 10.5h}\right]$ /500 pieces/h (7)

External failure cost per unit: 1.93566/piece/number of CCDs = $\left[\frac{Average\ whole-plant\ external\ failutre\ cost\ in\ January–September\ (691{,}032)}{20\ days \times 21\ h}\right]$/ $7CCDs/121SUM(FN = number\ of\ Type\ II\ errors)$ (8)

Internal failure cost per unit: 1.31865/piece/number of CCDs =$\left[\frac{Average\ whole-plant\ internal\ failutre\ cost\ in\ January–September\ (35{,}1622)}{20\ days \times 21\ h}\right]$/ $7CCDs/90\ SUM\ (TN = Number\ of\ defective\ units)$ (9)

TABLE 5. Total cost of turning on all CCDs given true defect rate and strictness level.

Strictness		Tight ← Strictness level of CCD → loose									
		10%	9%	8%	7%	6%	5%	4%	3%	2%	1%
True defect rate	10%	934.65	955.77	976.88	997.99	1019.11	1040.22	1061.34	1082.45	1103.56	1124.68
	9%	824.05	845.16	866.28	887.39	908.50	929.62	950.73	971.85	992.96	1014.07
	8%	815.15	737.61	755.67	776.79	797.90	819.01	840.13	861.24	882.36	903.47
	7%	815.15	737.61	660.07	666.18	687.30	708.41	729.52	750.64	771.75	792.87
	6%	815.15	737.61	660.07	582.53	576.69	597.81	618.92	640.04	661.15	682.26
	5%	815.15	737.61	660.07	582.53	504.99	487.20	508.32	529.43	550.55	571.66
	4%	815.15	737.61	660.07	582.53	504.99	427.45	397.71	418.83	439.94	461.06
	3%	815.15	737.61	660.07	582.53	504.99	427.45	349.91	307.81	327.77	347.74
	2%	815.15	737.61	660.07	582.53	504.99	427.45	349.91	272.37	218.73	239.85
	1%	815.15	737.61	660.07	582.53	504.99	427.45	349.91	272.37	194.83	129.24

Unit: RMB Per Hour
Note: The model suggests a strictness value for the lowest total inspection cost marked in a gray block

CCD strictness was close to the true defect rate, the total inspection cost is reduced. When the strictness was higher than the true defect rate, the frequency of overkills increased even though the system could reject more defective goods with reduced Type II error cost. Consequently, the costs of human reinspection due to Type I error, scrapping, and reworking increase. By contrast, when the strictness was lower than the best setting value, the leakage problem was aggravated and more defective goods were being sold to customers, thus increasing Type II error cost (i.e., customer complaints).

Figure 9 compares the total AOI costs of different strictness levels in the all-CCD-on mode with the defect rate fixed at 7%. The dotted line indicates the total cost of AOI in the all-CCD-off mode. Despite the different true defect rates, the initial AOI cost remained unchanged when the best strictness setting and lowest total inspection cost were identified. However, the probability of overkills and leakage varied when the strictness level changed, causing changes in the total inspection cost.

Compared with a rule-based AOI system (the CCD strictness is fixed at a constant), the AOI system is installed with an operationally best CCD strictness model (i.e., the model automatically recommends the best CCD strictness levels) exhibited greater cost-effectiveness. For example, when true defect rate is 7%, the proposed strictness model suggests to set strictness at 8% instead of 10%, the total inspection cost reduces from \$815.15 to \$660.07, which was \$ 155.08 (or 23.49%). By applying the strictness model, quality operators can adjust the AOI strictness setting based on production sampling yield and quality status.

The experiment results indicated that the closer the strictness level to the true defect rate is, the lower the total AOI cost is. For example, when the true defect rate was fixed at 7%, (i) the lowest inspection cost was identified when the strictness was set as 8%. (ii) Type II errors were less frequent than Type I errors when the strictness ranged from 8% to 10% under the all-CCD-on mode. (iii) When the strictness was <7%, Type II errors became costlier than the internal failure cost of Type I errors and increased when the strictness level decreased. The proposed AOI system with this study's

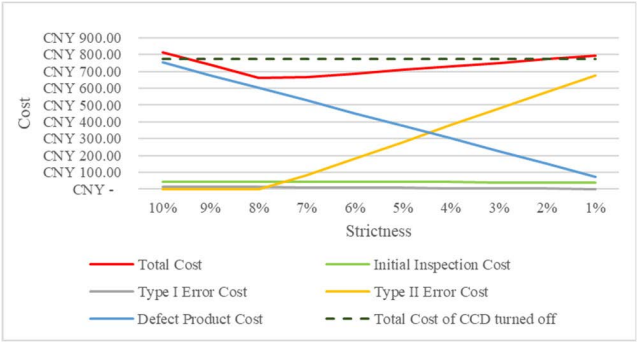

FIGURE 9. AOI cost changes with CCD strictness level when the true defect rate was set at 7%.

operational-level strictness model outperformed a rule-based AOI system in terms of cost-effectiveness. (iv) When the CCD strictness was set as 8% (true defect rate = 7%), the lowest total inspection cost was achieved. Conversely, when the strictness was inappropriately set such as 10%, the total cost per hour increased by 23.49%.

B. RESULT OF THE MULTI-CCD SWITCH MODEL

This section analyzes the cost-effectiveness of the proposed multi-CCD switch model. When the model detects that the total inspection cost in the CCD-on mode is higher than that in the CCD-off mode, the model suggests to the user to turn off certain CCDs. The best switch decisions in the CCD-on mode suggested by the proposed model in different strictness levels are described in Table 6. The result of multi-CCD switch model revealed that:

(i) When the strictness level was loose (1%–3%) with the true defect rate ranging 1%–10%, the multi-CCD switch model recommended turning off more than half the CCDs on most occasions because a CCD with excessively low strictness will not solve the problem of defect leakage and may cause an increase in costs related to Type II error, initial inspection, and defective goods.

(ii) When the strictness level ranged from 7% to 10% (with the true defect rate ranging from 1% to 10%), the switch model recommended turning off half the CCDs (Table 6a)

TABLE 6. The best multi-CCD switch decisions.

(a) Number of CCDs to turn on

True Defect Rate \ Strictness level	10%	9%	8%	7%	6%	5%	4%	3%	2%	1%
10%	7	5	5	5	5	5	3	2	2	2
9%	7	7	5	5	5	5	3	2	2	2
8%	7	7	7	5	5	5	4	2	2	2
7%	0	6	7	7	5	5	5	2	2	2
6%	0	0	3	7	7	5	5	3	2	2
5%	0	0	0	0	7	6	5	3	2	2
4%	0	0	0	0	0	5	5	5	2	2
3%	0	0	0	0	0	0	0	5	2	2
2%	0	0	0	0	0	0	0	0	3	2
1%	0	0	0	0	0	0	0	0	0	1

(b) Total cost of turning on CCDs

True Defect Rate \ Strictness level	10%	9%	8%	7%	6%	5%	4%	3%	2%	1%
10%	934.65	952.70	959.14	965.57	972.01	978.44	979.81	975.21	970.43	965.66
9%	824.05	845.16	860.92	867.35	873.78	880.22	883.92	880.26	875.48	870.70
8%	815.15	737.61	755.67	769.13	775.56	782.00	787.55	785.31	780.53	775.75
7%	774.23	737.56	660.07	666.18	677.34	683.78	690.21	690.36	685.58	680.80
6%	663.62	663.62	653.93	582.53	576.69	585.55	591.99	595.28	590.63	585.85
5%	553.02	553.02	553.02	553.02	504.99	487.15	493.77	499.39	495.68	490.90
4%	442.42	442.42	442.42	442.42	442.42	425.43	395.54	401.98	400.72	395.94
3%	327.95	327.95	327.95	327.95	327.95	327.95	327.95	302.79	303.11	298.01
2%	221.21	221.21	221.21	221.21	221.21	221.21	221.21	221.21	210.75	206.04
1%	110.60	110.60	110.60	110.60	110.60	110.60	110.60	110.60	110.60	110.24

Unit: RMB Per Hour

(C) The results of the two-stage model with defective rate 7%

Decision Model Phase	Result Model
Stage-I: The CCD strictness model	Set Value: 8%
Stage-II: The multi-CCD switch model	7 CCDs fully Open
Total Cost	660.07(CNY)

(D) The best multi-CCD switch decision given true defective rates (when the true defect rate is set to 7%)

CCD switch decision (strictness)	10%		9%		8%		7%		6%		5%		4%		3%		2%		1%	
	Sw-itch	Total cost	Sw-itch	Total cost	Sw-itch	Total cost	Sw-itch	Total cost	Sw-itch	Total cost	Sw-itch	Total cost	Sw-itch	Total cost	Sw-itch	Total cost	Sw-itch	Total cost	Sw-itch	Tota l cost
CCD1	0	63.58	1	61.92	1	55.67	1	61.37	0	63.58	0	63.58	0	63.58	0	63.58	0	63.58	0	63.58
CCD2	0	70.96	0	70.96	1	63.74	1	68.44	0	70.96	0	70.96	0	70.96	0	70.96	0	70.96	0	70.96
CCD3	0	174.59	1	160.39	1	143.20	1	137.96	1	134.87	1	131.77	1	128.67	1	125.57	1	122.48	1	119.38
CCD4	0	156.18	1	147.65	1	131.88	1	128.05	1	126.37	1	124.69	1	123.01	1	121.33	1	119.65	1	117.96
CCD5	0	104.02	1	98.18	1	87.90	1	89.57	1	93.39	1	97.21	1	101.02	0	104.02	0	104.02	0	104.02
CCD6	0	101.07	1	97.22	1	87.05	1	88.83	1	92.75	1	96.67	1	100.59	0	101.07	0	101.07	0	101.07
CCD7	0	103.83	1	101.24	1	90.62	1	91.95	1	95.43	1	98.91	1	102.38	0	103.83	0	103.83	0	103.83
Sum of CCDs to turn-on	0	774.23	6	737.56	7	660.07	7	666.18	5	677.34	5	683.78	5	690.21	2	690.36	2	685.58	2	680.80
Total cost in the all-CCDs-on mode	7	815.15	7	737.61	7	660.07	7	666.18	7	687.30	7	708.41	7	729.52	7	750.64	7	771.75	7	792.87
Inspection cost-effectiveness (by hour)	-	40.92	-	0.05	-	0	-	0	-	9.96	-	24.63		39.31	-	60.28	-	86.17	-	112.07
Inspection cost-effectiveness(%)	-	5.02%	-	0.006%	-	0	-	0	-	1.45%	-	3.48%		5.39%	-	8.03%	-	11.17%	-	14.13%

Unit: RMB Per Hour

most of time because overkills were likely at a high strictness level, which may in turn enhance the costs associated with defective scrapping, reworking, and Type I errors in human inspection.

(iii) Conversely, when the strictness was equal or close to the true defect rate, the model suggested turning on more than half the CCDs. As indicated in Table 6a, when the strictness level was close to true defect rate (i.e., when the two variables were both 6%, 7%, 8%, 9%, or 10%), the multi-CCD switch model recommended leaving all the seven CCDs open. When the strictness level and true defect rate were both 5%, 4%, or 3%, the model recommended turning on 6, 5, and 5 CCDs, respectively, because turning on more than half the CCDs helped reduce Type II error and maintain a lower Type I reinspection cost relative to Type II defect leakage cost; the model suggested turning off one or two CCDs because these CCDs did not help reduce Type II cost when they were on.

(iv) When the strictness level and true defect rate were both 1% or 2%, the multi-CCD switch model suggested opening only 1 or 3 CCDs, respectively, because a low true defect rate indicated improved process capability. When most of the CCDs were closed, the Type II cost remained lower than the AOI initial inspection cost and Type I error cost in most circumstances. Additionally, the remaining turned-on CCDs demonstrated favorable performance in defect detection, which in turn lowered the Type II cost and could compensate for costs for initial inspection and Type I error resolution. The aforementioned scenario indicated that the defect detection efficiency in CCDs was crucial in making switch decisions. For example, when the strictness level and true defect rate were both 1%, the switch model recommended turning on CCD3, rather than other cameras, because the efficiency of CCD3 in capturing defects (22.55%) was greater than that of its counterparts. In other words, turning on CCD3 was more cost-effective with reduced Type II error cost. Moreover, if the other CCDs were turned on, the reduced Type II cost could not compensate for the combined cost of initial inspection and Type I error reinspection. Therefore, the model recommended turning off all cameras except for CCD3.

(v) The analysis also confirmed the influence of CCD false call rate on multi-CCD switch decisions. When the strictness level and true defect rate were both 2%, the switch model recommended turning on CCD3, CCD4, and CCD5 because of their efficiency in defect detection (22.55%, 20.17%, and 13.44%, respectively). The model did not suggest turning on CCD6 and CCD7 (with similar efficiency [13.24% and 21.52%, respectively] to that of CCD5) because these two devices had higher false call rates (13.24% and 21.52% for CCD6 and CCD7, respectively) compared with other cameras. Further analysis demonstrated that although turning on CCD6 or CCD7 helped reduce Type II cost, the costs of initial inspection, Type I error reinspection, and defective goods collectively increased.

The cost-effectiveness of an AOI system installed with a strategic-level multi-CCD switch model was compared with that of an AOI system without such a model, at different true defect rates. As suggested in Table 5, (i) when the strictness level and true defect rate were set as 8% and 7%, respectively, the inspection cost of AOI in the all-CCD-on mode was the lowest, costing \$660.07/h. At the same true defect rate, the total cost increased to \$815.15/h at the strictness level of 10%. After the optimized multi-CCD switch model was installed, the total inspection cost could be reduced by 19.02%. Applications of the proposed strictness model can help flexibly adjust the AOI inspection strategy according to current quality conditions. (ii) In this 10%-strictness scenario (true defect rate = 7%), the multi-CCD switch model recommended turning off all the CCDs, resulting in a total AOI cost of \$774.23/h, which was 5.02% (\$40.92) less than the cost in the all-CCD-on mode (Table 6b). (iii) Furthermore, when the strictness level and true defect rate were set as 1% and 7%, respectively, when all CCDs were switched on, the total inspection cost was \$792.87/h, higher than the cost of \$660.07/h after the model-provided optimized switch decision was made (referring to Table 6d). When the strictness level was 8% under the all-CCD-on mode, the total inspection cost could be reduced by 20.12% after the best switch arrangement were implemented, with a rate of \$132.8/h. The total inspection Cost is 660.07 (Table 6c) (iv) When the strictness level was set as 1% (true defect rate = 7%), the multi-CCD switch model recommended turning off five CCDs (CCD1, CCD2, CCD5, CCD6, and CCD7); the suggestion helped reduce the total AOI cost from \$792.87 (all-CCD-on mode) to \$680.80, which was 14.13% less (i.e., saving \$112.07), creating the most favorable cost-effectiveness among the 1%–10% strictness levels. Under different strictness settings, a corresponding best lens switch combination can minimize total inspection cost.

V. CONCLUSION

This study proposed a two-stage decision model for the multi-CCD AOI system deployment. The proposed model is successfully implemented in an electrical connector manufacturing plant. The first stage of the model comprises an operational-level decision model that decides the single CCD strictness level. The second stage of the proposed AOI deployment model comprises a strategic-level CCD-switch decisions. The multi-CCD switch decision model suggests the best switch on/off decision of multiple CCDs. Defective products Reinspection procedure using deep learning CNN model. CNN classification model can be used to assist the existing AOI architecture. Providing a new option for back-end quality re-inspection.

As smart manufacturing becomes increasingly necessary and the electronics manufacturing industry become more competitive, AOI is expected to face greater challenges, such as more varied defects and inspection items and a shorter inspection time before the delivery date. The performance and accuracy of AOI systems are key to overcoming these challenges. Under these circumstances, the proposed multi-CCD AOI system deployment model for providing recommendations on multi-CCD switching is promising. The proposed two-stage model achieves flexible inspection settings and operations at low cost, and can be widely

implemented in different application scenarios of overkill and leakage problems.

Some future studies are recommended to focus on clarifying the interactive effects among defective types, CCD strictness, and multi-CCD switch decisions to overall AOI performances and applications of the proposed model long with manufacturing execution system.

REFERENCES

[1] W.-C. Wang, S.-L. Chen, L.-B. Chen, and W.-J. Chang, "A machine vision based automatic optical inspection system for measuring drilling quality of printed circuit boards," *IEEE Access*, vol. 5, pp. 10817–10833, 2017.

[2] M. Sony and S. Naik, "Critical factors for the successful implementation of industry 4.0: A review and future research direction," *Prod. Planning Control*, vol. 31, no. 10, pp. 799–815, Jul. 2020.

[3] M. A. Al Rahman and A. Mousavi, "A review and analysis of automatic optical inspection and quality monitoring methods in electronics industry," *IEEE Access*, vol. 8, pp. 183192–183271, 2020.

[4] Y. Liu and F. Yu, "Automatic inspection system of surface defects on optical IR-CUT filter based on machine vision," *Opt Lasers Eng.*, vol. 55, pp. 243–257, Apr. 2014.

[5] P. Helo and Y. Hao, "Artificial intelligence in operations management and supply chain management: An exploratory case study," *Prod. Planning Control*, pp. 1–18, Apr. 2021, doi: 10.1080/09537287.2021.1882690.

[6] T. Czimmermann, G. Ciuti, M. Milazzo, M. Chiurazzi, S. Roccella, C. M. Oddo, and P. Dario, "Visual-based defect detection and classification approaches for industrial applications—A survey," *Sensors*, vol. 20, no. 5 p. 1459, 2020.

[7] D. Honzátko, E. Türetken S. A. Bigdeli, L. A. Dunbar, and P. Fua, "Defect segmentation for multi-illumination quality control systems," *Mach. Vis. Appl.*, vol. 32, no. 6, pp. 1–16, Nov. 2021.

[8] S. Yammen and P. Muneesawang, "An advanced vision system for the automatic inspection of corrosions on pole tips in hard disk drives," *IEEE Trans. Compon., Packag., Manuf. Technol.*, vol. 4, no. 9, pp. 1523–1533, Sep. 2014.

[9] R. Miao, Z. Jiang, Q. Zhou, Y. Wu, Y. Gao, J. Zhang, and Z. Jiang, "Online inspection of narrow overlap weld quality using two-stage convolution neural network image recognition," *Mach. Vis. Appl.*, vol. 32, no. 1, pp. 1–14, Jan. 2021.

[10] M. Ojer, "Real-time automatic optical system to assist operators in the assembling of electronic components," *Int. J. Adv. Manuf. Technol.*, vol. 107, no. 5, pp. 2261–2275, 2020.

[11] Z. Seyedghorban, H. Tahernejad, R. Meriton, and G. Graham, "Supply chain digitalization: Past, present and future," *Prod. Planning Control*, vol. 31, nos. 2–3, pp. 96–114, Feb. 2020.

[12] T. Takacs and L. Vajta, "Novel outlier filtering method for AOI image databases," *IEEE Trans. Compon., Packag., Manuf. Technol.*, vol. 2, no. 4, pp. 700–709, Apr. 2012.

[13] Y. Han, J. Fan, and X. Yang, "A structured light vision sensor for on-line weld bead measurement and weld quality inspection," *Int. J. Adv. Manuf. Technol.*, vol. 106, nos. 5–6, pp. 2065–2078, Jan. 2020.

[14] J. M. Runji and C.-Y. Lin, "Markerless cooperative augmented reality-based smart manufacturing double-check system: Case of safe PCBA inspection following automatic optical inspection," *Robot. Comput.-Integr. Manuf.*, vol. 64, Aug. 2020, Art. no. 101957.

[15] S. Mandroli, A. K. Shrivastava, and Y. Ding, "A survey of inspection strategy and sensor distribution studies in discrete-part manufacturing processes," *IIE Trans.*, vol. 38, no. 4, pp. 309–328, 2006.

[16] M. A. Farooq, R. Kirchain, H. Novoa, and A. Araujo, "Cost of quality: Evaluating cost-quality trade-offs for inspection strategies of manufacturing processes," *Int. J. Prod. Econ.*, vol. 188, pp. 156–166, Jun. 2017.

[17] A. Salado and H. Kannan, "A mathematical model of verification strategies," *Syst. Eng.*, vol. 21, no. 6, pp. 593–608, Nov. 2018.

[18] P. Zheng, H. Wang, Z. Sang, R. Y. Zhong, Y. Liu, C. Liu, K. Mubarok, S. Yu, and X. Xu, "Smart manufacturing systems for industry 4.0: Conceptual framework, scenarios, and future perspectives," *Frontiers Mech. Eng.*, vol. 13, no. 2, pp. 137–150, Jun. 2018.

[19] T.-H. Sun, F.-C. Tien, F.-C. Tien, and R.-J. Kuo, "Automated thermal fuse inspection using machine vision and artificial neural networks," *J. Intell. Manuf.*, vol. 27, no. 3, pp. 639–651, Jun. 2016.

[20] D. Yapi, M. Mejri, M. S. Allili, and N. Baaziz, "A learning-based approach for automatic defect detection in textile images," *IFAC-PapersOnLine*, vol. 48, no. 3, pp. 2423–2428, 2015, doi: 10.1016/j.ifacol.2015.06.451.

[21] N. G. Shankar and Z. W. Zhong, "A rule-based computing approach for the segmentation of semiconductor defects," *Microelectron. J.*, vol. 37, no. 6, pp. 500–509, Jun. 2006.

[22] Y. Yang, Z.-J. Zha, M. Gao, and Z. He, "A robust vision inspection system for detecting surface defects of film capacitors," *Signal Process.*, vol. 124, pp. 54–62, Jul. 2016.

[23] J. Chen and X. Ran, "Deep learning with edge computing: A review," *Proc. IEEE*, vol. 107, no. 8, pp. 1655–1674, Aug. 2019.

[24] R. Huang, J. Gu, X. Sun, Y. Hou, and S. Uddin, "A rapid recognition method for electronic components based on the improved YOLO-V3 network," *Electronics*, vol. 8, no. 8, p. 825, Jul. 2019.

[25] S. C. Horng, F. Y. Yang, and S. S. Lin, "Applying PSO and OCBA to minimize the overkills and re-probes in wafer probe testing," *IEEE Trans. Semicond. Manuf.*, vol. 25, no. 3, pp. 531–540, Aug. 2012.

[26] M. Abadi *et al.*, "TensorFlow: Large-scale machine learning on heterogeneous distributed systems," 2016, *arXiv:1603.04467*.

[27] J. Cheng, J. Wu, C. Leng, Y. Wang, and Q. Hu, "Quantized CNN: A unified approach to accelerate and compress convolutional networks," *IEEE Trans. Neural Netw. Learn. Syst.*, vol. 29, no. 10, pp. 4730–4743, Oct. 2018.

[28] Y. Iwahori, Y. Takada, T. Shiina, Y. Adachi, M. K. Bhuyan, and B. Kijsirikul, "Defect classification of electronic board using dense SIFT and CNN," *Proc. Comput. Sci.*, vol. 126, pp. 1673–1682, Jan. 2018.

[29] M. Zhang, J. Wu, H. Lin, P. Yuan, and Y. Song, "The application of one-class classifier based on CNN in image defect detection," *Proc. Comput. Sci.*, vol. 114, pp. 341–348, Jan. 2017.

KUNG-JENG WANG (Member, IEEE) received the Ph.D. degree in industrial engineering from the University of Wisconsin at Madison. He is currently a Professor and the Head of the Department of Industrial Management, National Taiwan University of Science and Technology (Taiwan Tech). He works closely with industries for research on manufacturing management and resource portfolio planning. He has published about 100 academic articles in international academic journals, such as IEEE TRANSACTIONS ON SYSTEMS, MAN, AND CYBERNETICS, *IIE Transactions*, *European Journal of Operational Research*, the *International Journal of Production Research*, and the journal of *Robotics and CIM*. His current research interests include intelligent production systems and value chain management.

YI-CHENG QIU is currently pursuing the Ph.D. degree with the Department of Industrial Management, National Taiwan University of Science and Technology. His current research interests include smart manufacturing and automatic optical inspection.